Comparison of low- and ultralow-dose computed tomography protocols for quantitative lung and airway assessment

Emily Hammond
Department of Radiology, University of Iowa Hospitals and Clinics, 200 Hawkins Drive, Iowa City, IA 52242, USA
Department of Biomedical Engineering, University of Iowa, 1402 Seamans Center, Iowa City, IA 52242, USA

Chelsea Sloan
Department of Radiology, University of Iowa Hospitals and Clinics, 200 Hawkins Drive, Iowa City, IA 52242, USA

John D. Newell Jr.
Department of Radiology, University of Iowa Hospitals and Clinics, 200 Hawkins Drive, Iowa City, IA 52242, USA
Department of Biomedical Engineering, University of Iowa, 1402 Seamans Center, Iowa City, IA 52242, USA

Jered P. Sieren
Imaging services, VIDA Diagnostics, Inc., 2500 Crosspark Road, W250 BioVentures Center, Coralville, IA 52241, USA

Melissa Saylor
Department of Radiology, University of Iowa Hospitals and Clinics, 200 Hawkins Drive, Iowa City, IA 52242, USA

Craig Vidal
Imaging services, VIDA Diagnostics, Inc., 2500 Crosspark Road, W250 BioVentures Center, Coralville, IA 52241, USA

Shayna Hogue, Frank De Stefano, and Alexa Sieren
Department of Radiology, University of Iowa Hospitals and Clinics, 200 Hawkins Drive, Iowa City, IA 52242, USA

Eric A. Hoffman
Department of Radiology, University of Iowa Hospitals and Clinics, 200 Hawkins Drive, Iowa City, IA 52242, USA
Department of Biomedical Engineering, University of Iowa, 1402 Seamans Center, Iowa City, IA 52242, USA
Department of Medicine, University of Iowa Hospitals and Clinics, 200 Hawkins Drive, Iowa City, IA 52242, USA

Jessica C. Sieren[a)]
Department of Radiology, University of Iowa Hospitals and Clinics, 200 Hawkins Drive, Iowa City, IA 52242, USA
Department of Biomedical Engineering, University of Iowa, 1402 Seamans Center, Iowa City, IA 52242, USA

(Received 30 January 2017; revised 19 June 2017; accepted for publication 21 June 2017; published 2 August 2017)

Purpose: Quantitative computed tomography (CT) measures are increasingly being developed and used to characterize lung disease. With recent advances in CT technologies, we sought to evaluate the quantitative accuracy of lung imaging at low- and ultralow-radiation doses with the use of iterative reconstruction (IR), tube current modulation (TCM), and spectral shaping.
Methods: We investigated the effect of five independent CT protocols reconstructed with IR on quantitative airway measures and global lung measures using an *in vivo* large animal model as a human subject surrogate. A control protocol was chosen (NIH-SPIROMICS + TCM) and five independent protocols investigating TCM, low- and ultralow-radiation dose, and spectral shaping. For all scans, quantitative global parenchymal measurements (mean, median and standard deviation of the parenchymal HU, along with measures of emphysema) and global airway measurements (number of segmented airways and pi10) were generated. In addition, selected individual airway measurements (minor and major inner diameter, wall thickness, inner and outer area, inner and outer perimeter, wall area fraction, and inner equivalent circle diameter) were evaluated. Comparisons were made between control and target protocols using difference and repeatability measures.
Results: Estimated CT volume dose index (CTDIvol) across all protocols ranged from 7.32 mGy to 0.32 mGy. Low- and ultralow-dose protocols required more manual editing and resolved fewer airway branches; yet, comparable pi10 whole lung measures were observed across all protocols. Similar trends in acquired parenchymal and airway measurements were observed across all protocols, with increased measurement differences using the ultralow-dose protocols. However, for small airways (1.9 ± 0.2 mm) and medium airways (5.7 ± 0.4 mm), the measurement differences across all protocols were comparable to the control protocol repeatability across breath holds. Diameters, wall thickness, wall area fraction, and equivalent diameter had smaller measurement differences than area and perimeter measurements.
Conclusions: In conclusion, the use of IR with low- and ultralow-dose CT protocols with CT volume dose indices down to 0.32 mGy maintains selected quantitative parenchymal and airway

measurements relevant to pulmonary disease characterization. © *2017 American Association of Physicists in Medicine* [https://doi.org/10.1002/mp.12436]

Key words: airway measurements, chronic obstructive pulmonary disease, low-dose computed tomography, lung disease assessment, quantitative CT protocols

1. INTRODUCTION

Quantitative computed tomography (CT) measures are increasingly being developed and used to characterize lung disease, such as asthma[1–4] and chronic obstructive pulmonary disease (COPD),[5–7] with baseline measurements established in healthy, nonsmoking adults.[8] However, accuracy and repeatability of quantitative measures have previously been shown to be sensitive to a wide range of variables.[9] We have previously reported on considerations for developing quantitative CT lung protocols to minimize variability in quantitative measures.[10] These recommendations have applications to CT lung protocol development for multicenter trials for consistent acquisition of high-quality quantitative subject data across multiple institutions and multiple scanner technologies, with the most recent development of the subpopulations and intermediate outcome measures in COPD (SPIROMICS) CT protocol.[11,12]

Incorporation of recent CT technologies allow for comparable qualitative CT data with a significant reduction in dose. The use of tube current modulation (TCM), characterized by automatic adjustment of the tube current based on patient size and tissue attenuation characteristics, has been shown to reduce dose while maintaining image quality.[13–16] Iterative reconstruction (IR) has also been used to maintain qualitative image integrity in conjunction with low-dose protocols.[17–19] Recent addition of spectral shaping capabilities, via the addition of tin filtering, increases the mean energy of the x-ray spectrum. The removal of low-energy x-ray, which contribute minimally to CT data quality, has shown utility in dose reduction in pulmonary nodule detection in chest CT,[20] in higher body weight patients,[21] and pediatric imaging.[22] Previously, low-dose protocols have allowed for imaging down to 0.3 mSv while preserving quantitative accuracy of density metrics assessed in a test object simulating a range of thoracic-based densities.[23]

Multiple multicenter studies, including SPIROMICS,[11] the Chronic Obstructive Pulmonary Disease Genetic Epidemiology Study (COPDGene),[24] the Severe Asthma Research Project (SARP),[25] and the Multi-Ethnic Study of Atherosclerosis (MESA) Lung study,[26] incorporate quantitative indices of lung structure derived from CT. These quantitative CT measures include percent emphysema (percent of lung less than −950 HU or −910 HU on inspiratory CT scans) and percent air trapping (percent of lung less than −856 HU on expiratory CT scans), and measures of airway geometry at multiple airway generations such as wall area percent, wall thickness, luminal diameter, and inner luminal perimeter measurements. The square root of wall area for a theoretical bronchus with 10 mm lumen inner perimeter (pi10) is a standardized measure of airway wall thickening which facilitates the evaluation of airway wall changes across subjects with different-sized lungs/airways,[27,28] with utility demonstrated in COPD,[29,30] and pulmonary hypertension.[31] The success of these studies and other studies in characterizing emphysema, small airway disease, and airway geometry have been recognized although there is concern that the radiation dose may be a limiting factor in applying quantitative CT to the characterization and longitudinal monitoring of several lung diseases. The current study was designed to look at the effects of low-dose and ultralow-dose CT scanning using a state of the art CT scanner to see how lung density and airway geometry measures are affected by decreasing the dose in a large animal model. It is the goal of this work to inform researchers' choice of CT scan parameters that affect dose in human subjects. This will also help inform the translation of these multicenter research studies to the more widespread applications of these promising research findings to the individual clinical patient.

In this paper, we investigate the effect of five independent CT protocols reconstructed with IR on *in vivo* quantitative airway measures and global lung measures. Protocols incorporate TCM, low-dose and ultralow-dose protocols, and tin filtering applied with a single source. We report on the comparison of measures obtained from a control protocol and each independent protocol using an animal model. We also investigate the repeatability of acquired measures from each protocol across multiple scans.

2. MATERIALS AND METHODS

All procedures were approved for by the Institutional Animal Care and Use Committee (IACUC). A male swine, 39 kg, was placed under anesthesia, induced with a mixture of telazol (2.2 mg/kg), ketamine (1.1 mg/kg), and xylazine (1.1 mg/kg) and maintained with isoflurane (1%–3%). The animal was intubated and placed in the supine position in the isocenter of the CT scanner. Mechanical ventilation was performed with a respiratory rate of 10–16 breaths per minute with a tidal volume of 10 mL/kg and a positive end-expiratory pressure (PEEP) of 5 cm H_2O. Enforced breath holds were utilized during imaging to remove respiratory motion and maintained at a PEEP of 25 cm H_2O with a water column. Monitoring was performed with electrocardiogram (ECG), oxygen saturation pressure (SP-O_2), and end tidal carbon dioxide pressure (ET-CO_2). Anesthesia and ventilation parameters were adjusted to maintain an ECG between 80 and 100 beats per minutes, an SP-O_2 of 99%–100%, and an ET-CO_2 between 35 and 45 mmHg.

Imaging was performed with a Siemens SOMATOM Force CT scanner (Siemens Healthcare, Forchheim, Germany) using five independent protocols ranging in estimated

CT volume dose index (CTDIvol) from 7.32 mGy to 0.32 mGy, with parameters listed in Table I. The designated National Institutes of Health (NIH) SPIROMICS study protocol with the addition of TCM ("CARE Dose") was chosen as a control protocol with variability assessed within the protocol. The corresponding quality reference tube current time product (mAs) was chosen to match a target CTDIvol of 7.32 mGy. The control protocol was then compared with the current NIH-SPIROMICS CT Protocol which does not incorporate TCM,[11,12] a low-dose chest protocol recommended by the manufacturer, an ultralow-dose protocol without incorporating tin filtering, and an ultralow-dose protocol recommended for the Force scanner with the use of tin filtering.

Prior to imaging, pulmonary recruitment was performed with a PEEP of 12–14 cmH_2O for 2 min. Volumes were acquired in sets of three acquisitions in a single 30-s inspiratory breath hold. For each set, a volume was acquired with the control protocol followed by two acquisitions with a target protocol, as listed in Table I. Each acquisition set concluded with 5 min of ventilation with a PEEP of 5 cmH_2O to ensure return to baseline pulmonary function. The animal respiration and CT acquisition schema is illustrated in Fig. 1. All volumes were reconstructed with the same parameters and standardized field of view for comparison: Qr40 kernel, level 5 IR (SAFIRE), field of view diameter 250 mm, and resolution of 0.49 mm × 0.49 mm × 0.75 mm.

Quantitative analysis was performed with lung parenchymal and airway measurements. Lung segmentations were generated on all control protocol volumes acquired with an intensity-based segmentation algorithm using in-house software (Pulmonary Analysis Software Suite[32]) for a total of five segmentations. Lung segmentations were visually confirmed and manual editing was performed if required to exclude airways and vessels. Quantitative values were obtained by applying the lung segmentation generated from the control volume to the two target volumes taken in the corresponding breath hold. Global mean, median, and standard deviation measurements, along with percent emphysema

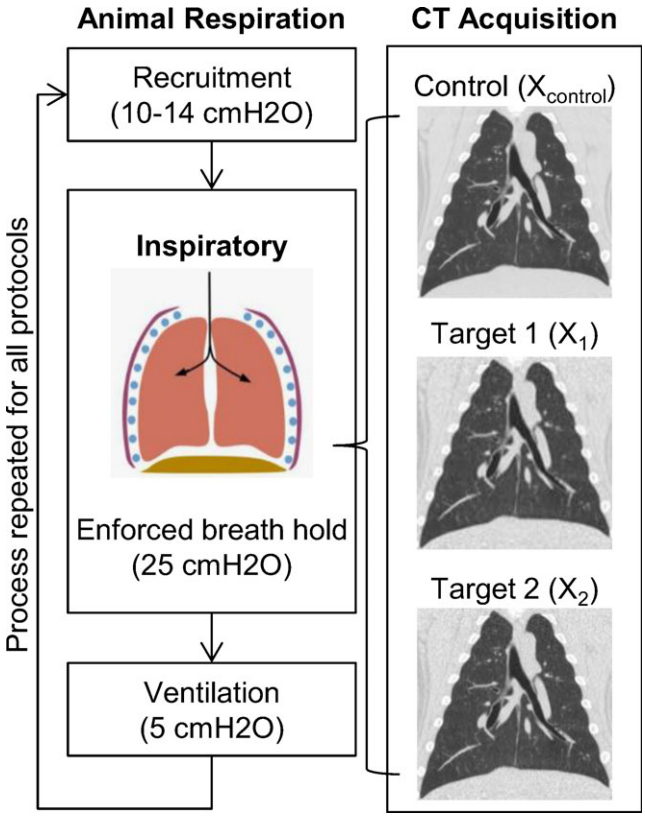

FIG. 1. CT Data Acquisition Summary. For each inspiratory lung volume, three CT datasets were acquired in a single enforced breath hold — one control CT scan followed immediately by two target CT scans. Each breath hold was preceded by 2 min of recruitment and followed by 5 min of normal ventilation. This process of CT data collection was repeated for all protocols. [Color figure can be viewed at wileyonlinelibrary.com]

TABLE I. Description of the image acquisition parameters used to compare five computed tomography imaging protocols. Each set was acquired in a single breath hold with the control protocol ($X_{control}$) acquired first followed by two target protocols (X_1, X_2). All images were reconstructed with the same iterative reconstruction kernel, same field of view diameter, and same voxel resolution.

Scan ID	Scan description	Quality reference mAs	kV	Tube current modulation ("CARE Dose")	Pitch	Exp. time
Control variability	Control	118	120	On	1	0.5
	SPIROMICS w TCM	118	120	On	1	0.5
	SPIROMICS w TCM	118	120	On	1	0.5
No-TCM	Control	118	120	On	1	0.5
	SPIROMICS	110	120	Off	1	0.5
	SPIROMICS	110	120	Off	1	0.5
Low-dose	Control	118	120	On	1	0.5
	Low-dose chest	52	110	On	1.2	0.5
	Low-dose chest	52	110	On	1.2	0.5
Ultralow-dose	Control	118	120	On	1	0.5
	Ultralow-dose	10	120	On	1	0.5
	Ultralow-dose	10	120	On	1	0.5
Tin-filtered ultralow-dose	Control	118	120	On	1	0.5
	Sn ultralow-dose	97	Sn100	On	1.2	0.5
	Sn ultralow-dose	97	Sn100	On	1.2	0.5

(percent < -910 HU, percent < -950 HU) of lung parenchymal Hounsfield Units (HU) were calculated with the final segmentations. Performance of each protocol with reference to the control protocol was assessed via difference measures between volumes obtained in a single breath hold to determine the presence of a HU shift compared to the control protocol. Raw values were reported as the average across all control protocols.

Comparisons of airway measures were also performed to determine the effect each target protocol had on airway measurements compared to the control protocol. Airway trees were segmented and quantitative measurements were acquired using the APOLLO software (VIDA Diagnostics, Inc., Coralville, IA, USA). Editing was applied via seed point placement to fully extend the airway trees in the base of the lung to account for extended length of the pig lung. Airway segmentations were then assessed to ensure consistent branching structure across all acquired segmentations with merging of fractured branches occurring when required. The number of segmented airways was calculated post-editing and the pi10 value was obtained as a global comparative measure using all segmented airway branches.

Specific airway analysis was performed with quantitative measures generated for eight chosen airways, four medium sized (minor inner diameter 4–10 mm, inner area 20–40 mm^2), and four small sized (minor inner diameter < 4 mm, inner area < 20 mm^2), as shown in Fig. 2. Measurements included the minor and major inner diameter, wall thickness, inner and outer area, inner and outer perimeter, wall area percent (outer area – inner area/outer area), and inner equivalent circle diameter (inner perimeter/π). Evaluation was performed with difference measures between each target protocol and the corresponding control protocol obtained in the same breath hold. The magnitude of each difference was reported and averaged over medium airways and small airways for a single protocol to assess the deviations from control by type of airway. Comparisons were performed evaluating protocol effect on the acquired measurements and chosen airways. Cumulative change from control was also reported summing the mean difference magnitudes from all measurement across protocol and from all protocols across all measurements providing a global assessment for protocol and airway measurements. Raw values were reported as the average across all control protocols.

Additional analysis was performed to determine the presence of a bias within each protocol. Normal variability was determined for medium and small airways from the difference measures obtained with the control variability acquisitions. Minimum and maximum deviations were calculated with three standard deviations from zero and used as criterion to determine the number of airway difference measures outside of this range. Trends were observed to determine a systematic overestimation or underestimation of airway measurements within a specific protocol with reference to the control protocol.

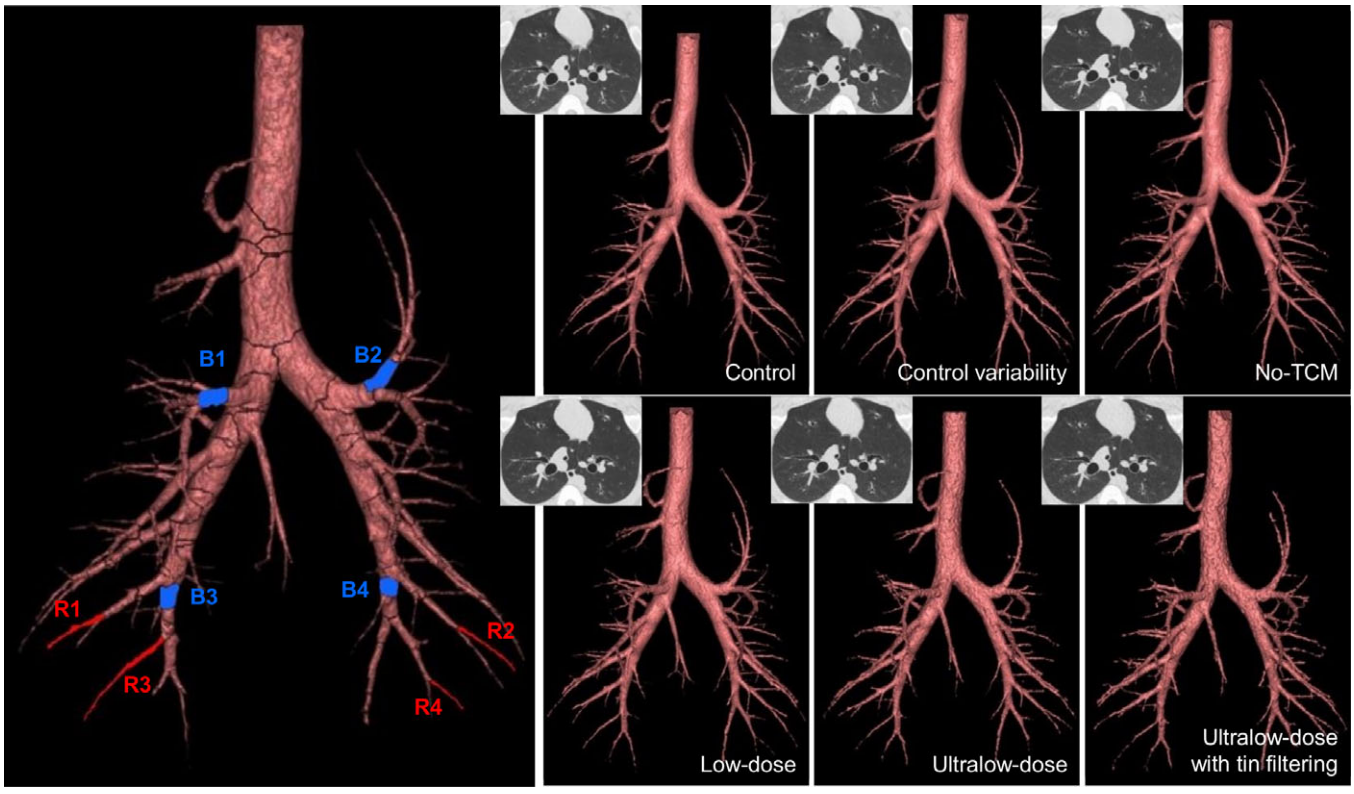

FIG. 2. Airway tree segmentations. The left most airway tree illustrates the eight airways isolated for analysis. Blue (BX) denotes the medium-sized airways, while red (RX) denotes the small airways. The remaining airway trees represent the segmented airway trees from all acquired protocols, denoted in the lower right corner of each image, with a corresponding CT cross section in the upper left corner.

Changes due to breath hold alone (consistent control protocol) were additionally determined to provide a baseline figure for comparison of acquired measurements obtained within a single breath hold. In each case, the breath hold was mechanically enforced using a PEEP of 20 cmH_2O. Differences were calculated between the control protocol acquired for each breath hold and the control protocol acquired for the first breath hold (control variability). Differences were reported in the same manner as previously stated for specific airway analysis.

Repeatability measurements were similarly obtained and evaluated to determine the ability to acquire consistent and reproducible quantitative measures. Difference measures were calculated between the two target protocols acquired in the same breath hold for parenchymal and airway measures. Averages were calculated for the medium airways and small airways. Differences were reported in the same manner as previously stated for parenchymal measures and global and specific airway measures. These results were placed into context of repeatability with a consistent acquisition protocol, but across mechanically enforced breath holds.

3. RESULTS

A total of five sets of three volumes per breath hold (one control and two target) were acquired in five separate breath holds, as illustrated in Fig. 1. CTDIvol for the control protocol ranged from 6.95 mGy to 7.02 mGy between all five sets of scans with an effective mAs of 104–105. This was compared to a quality reference mAs of 118, which represented the effective mAs required for an average-sized subject (70–80 kg). In comparison, no-TCM showed a 5% increase in CTDIvol (110 mAs, 7.32 mGy). The low-dose protocol showed a 64% reduction in CTDIvol (47 mAs, 2.48 mGy). The ultralow-dose protocol showed a 90.5% reduction (10 mAs, 0.67 mGy), while the tin-filtered ultralow-dose protocol demonstrated a 95% reduction (93 mAs, 0.32 mGy), as detailed in Table II. Consistent lung volumes were observed across scans acquired in a single breath hold, except within the control variability set, in which a 60 mL difference was observed between the control protocol lung volume (1.83 L) and the second target protocol lung volume (1.77 L). Therefore, for the control variability set, analysis was performed with the control and first target volume only.

3.A. Global parenchymal results

Lung segmentations were successfully generated for all control volumes and visually confirmed to match all scans taken within a breath hold. A separate segmentation was acquired for the first target volume in the control variability set due to the differences in observed lung volume. Global lung mean, median, and standard deviation did not appear to be affected by the deactivation of TCM, the use of low and ultralow-dose protocols, or tin filtering when using IR, as displayed in Table III. Differences between the target protocol and control protocols for global mean were largest (6.64 HU) with the low-dose protocol, while the largest standard deviation (4.21 HU) was incurred with the tin-filtered ultralow-dose protocol, and the maximum shift in median (5 HU) occurred for multiple acquisition protocols (no-TCM, low-dose, and tin-filtered ultralow-dose). All protocols showed the ability to acquire repeatable measurements (X_2–X_1) with the greatest variability observed in the low-dose protocol; however, all differences were well within the variability observed across breath holds.

Minimal differences were observed for percent emphysema for control variability and no-TCM protocols with repeatability comparable to that achieved across breath holds. Increased differences of approximately 1% were observed with the low-dose protocol, while the ultralow-dose and tin-filtered ultralow-dose protocols showed differences between

TABLE II. Parameters used during volume acquisition with corresponding CTDIvol and lung volumes and the results of global airway analysis. Dose reduction was calculated comparing the CTDIvol of the control protocol with the corresponding target protocol. Following airway segmentation, the number of airways was reported and pi10 was calculated. Lung volumes were determined from the final lung segmentation.

Scan ID	Scan description	Effective mAs	CTDIvol [mGy]	% reduction	# segmented airways	pi10	Lung volume [L]
Control variability	Control	105	7.02	–	262	3.71	1.83
	SPIROMICS w TCM	105	7.02	0%	243	3.71	1.81
No-TCM	Control	104	6.95	–	309	3.65	2.03
	SPIROMICS	110	7.32	−5%	332	3.66	2.03
	SPIROMICS	110	7.32	−5%	334	3.65	2.03
Low-dose	Control	104	6.99	–	303	3.65	1.99
	Low-dose chest	47	2.48	65%	306	3.68	1.99
	Low-dose chest	47	2.48	65%	311	3.66	1.99
Ultralow-dose	Control	105	7.02	–	320	3.68	2.05
	Ultralow-dose	10	0.67	90%	287	3.90	2.05
	Ultralow-dose	10	0.64	91%	256	3.84	2.05
Tin-filtered ultralow-dose	Control	104	6.95	–	322	3.67	2.02
	Sn ultralow-dose	93	0.32	95%	261	3.69	2.02
	Sn ultralow-dose	93	0.32	95%	249	3.76	2.02

TABLE III. Global parenchymal results. Difference measures comparing parenchymal values between control and target protocols and between the two target protocols acquired for the mean, median, standard deviation, and percent emphysema (% < −910 HU). Values were not reported for the second target volume for the control variability set indicated with an n/a.

	Mean (HU)			Median (HU)			Standard deviation (HU)			% < −910 HU (%)		
Average across all control protocols	−814.25 ± 10.38			−836.6 ± 7.47			86.47 ± 9.31			0.40 ± 0.09		
Protocol	X_1–X_c	X_2–X_c	X_2–X_1	X_1–X_c	X_2–X_c	X_2–X_1	X_1–X_c	X_2–X_c	X_2–X_1	X_1–X_c	X_2–X_c	X_2–X_1
Control variability	−1.06	n/a	n/a	0.00	n/a	n/a	−1.49	n/a	n/a	0.11	n/a	n/a
No-TCM	−2.60	−4.96	2.37	−2.00	−5.00	3.00	−0.24	−1.46	1.22	0.11	0.21	−0.10
Low-dose	−2.00	−6.64	4.63	−1.00	−5.00	4.00	−0.03	−1.92	1.89	0.90	1.26	−0.36
Ultralow-dose	0.68	−1.14	1.82	3.00	1.00	2.00	1.08	0.65	0.43	2.07	2.29	−0.22
Tin-filtered ultralow-dose	1.90	0.19	1.71	5.00	2.00	3.00	2.91	4.21	−1.31	2.97	3.03	−0.06

2% and 3% indicating the presence of a histogram shift at low intensities. Overall, the tin-filtered ultralow-dose had superior repeatability compared to all the other protocols for this measure. Minimal differences of less than 0.01% were reported comparing percent of voxels below −950 HU for control variability, no-TCM, and low-dose protocols compared to control. Further evidence of a histogram shift with ultralow-dose and tin-filtered ultralow-dose was seen with increased differences of 0.1% and 0.2%, respectively, for percent below −950 HU.

3.B. Global airway results

Fifteen airway segmentations were generated, edited, and visually confirmed to have consistent branching structure, seen in Fig. 2, for all volumes with calculated pi10 results shown in Table II. Ultralow-dose and tin-filtered ultralow-dose protocols showed increased fracturing in branching structure requiring more merging to ensure consistent branching. They also had fewer resolved airway branches compared to the corresponding control relative to the control variability, no-TCM, and low-dose protocols. The control variability set resulted in the least number of overall segmented airways, and also showed the smallest lung volumes potentially due to the order of set acquisition for the study and progressive recruitment/lung inflation over time. This is reflected by noting the number of airways segmented using the control protocol across the different breath holds increased from 262 to 322. The low-dose protocol showed the most consistent results with respect to the corresponding control, while the ultralow-dose protocols showed the greatest disparity (less) from control. Overall, the number of segmented airways had minimal effect on pi10 for the control variability, no-TCM, low-dose, and tin-filtered ultralow-dose protocols with difference magnitudes less than 0.10 from control. Larger differences (0.16 and 0.22) were observed with the ultralow-dose protocol; however, these are still within 6% of the corresponding control value.

3.C. Specific airway results

Eight airways were chosen for specific airway measurement analysis, divided into medium or small airways as defined across all control protocols acquired. The four medium airways had an average minor inner diameter of 5.70 ± 0.35 mm and inner area of 31.56 ± 4.27 mm^2. The four small airways had an average minor inner diameter of 1.93 ± 0.21 mm and inner area of 3.85 ± 0.80 mm^2.

3.C.1. Small airways

Major and minor inner diameter, wall thickness, inner perimeter, inner area, wall area percent, and inner equivalent circle diameter did not appear to be affected by change in protocol in small airways when compared to equivalent measures observed in the control variability results, as seen in Table IV. For outer perimeter and outer area, all protocols showed greater average difference magnitudes compared to the control variability protocol; however, average difference magnitudes were similar to those seen across breath holds for no-TCM and low-dose protocols. Average difference magnitudes greater than those seen across breath holds were observed for both ultralow-dose protocols for outer perimeter and outer area. Overall, average difference magnitudes were subvoxel (0.49 mm) or near subvoxel across most measurements. Similar trends were observed across cumulative change plots seen in Fig. 3.

Repeatability of small airway measurements, also presented in Table IV and Fig. 3, show repeatability comparable to the control protocol (control variability set) for minor and major inner diameter, wall thickness, inner perimeter, inner area, wall area percent, and inner equivalent circle diameter. Outer perimeter showed similar repeatability in low-dose and both ultralow-dose protocols with mildly elevated average difference magnitudes compared to those seen with control variability and no-TCM. Overall, the absence of TCM (no-TCM) produced the most repeatable results most likely explained by the lack of variability in the tube current.

Lastly, both ultralow-dose protocols showed presence of systematic overestimation of small airway measures using the variability observed in the control protocol. Additionally, outer area and outer perimeter were more likely to be overestimated across all protocols, suggesting difficulty in consistent segmentation of the outside of the airway.

TABLE IV. Specific airway results for small airways. Average difference magnitudes for the four analyzed small airways showing comparison of differences between each target scan and control scan acquired within the same breath hold (comparison to control) and differences between each target scan acquired within the same breath hold to assess for repeatability of airway measures (repeatability). Across breath hold differences are obtained between each control scan and the control scan acquired for the control variability set. Raw measurements were calculated from the airway measures obtained across each control scan. Results are presented as average difference magnitudes ± standard deviation. Bold indicates results showing the largest average difference magnitudes in comparison to control and across breath holds.

	Minor inner diameter (mm)	Major inner diameter (mm)	Wall thickness (mm)	Inner perimeter (mm)	Outer perimeter (mm)	Inner area (mm^2)	Outer area (mm^2)	Wall area percent	Inner equivalent circle diameter (mm)
Raw measurement	1.93 ± 0.21	2.48 ± 0.27	0.93 ± 0.07	7.23 ± 0.71	**13.37 ± 0.89**	3.85 ± 0.80	**13.65 ± 1.98**	0.72 ± 0.02	2.30 ± 0.23
Across breath holds	0.08 ± 0.06	0.11 ± 0.07	0.07 ± 0.06	0.28 ± 0.17	**0.19 ± 0.11**	0.27 ± 0.16	**0.47 ± 0.27**	0.03 ± 0.02	0.09 ± 0.05
Control variability	0.10 ± 0.05	0.10 ± 0.08	0.06 ± 0.06	0.29 ± 0.26	**0.11 ± 0.13**	0.28 ± 0.26	**0.24 ± 0.30**	0.03 ± 0.03	0.09 ± 0.08
Comparison to control ($X_{1/2}$–X_c)									
No-TCM	0.09 ± 0.05	0.08 ± 0.05	0.03 ± 0.03	0.21 ± 0.12	**0.22 ± 0.13**	0.23 ± 0.13	**0.48 ± 0.27**	0.01 ± 0.01	0.07 ± 0.04
Low-dose	0.07 ± 0.06	0.08 ± 0.07	0.05 ± 0.04	0.18 ± 0.21	**0.22 ± 0.16**	0.23 ± 0.26	**0.51 ± 0.45**	0.01 ± 0.01	0.06 ± 0.07
Ultralow-dose	0.11 ± 0.08	0.14 ± 0.11	0.06 ± 0.03	0.34 ± 0.35	**0.50 ± 0.50**	0.39 ± 0.39	**1.15 ± 1.05**	0.01 ± 0.01	0.11 ± 0.11
Sn ultralow-dose	0.07 ± 0.04	0.11 ± 0.10	0.08 ± 0.04	0.29 ± 0.24	**0.54 ± 0.30**	0.25 ± 0.23	**1.11 ± 0.66**	0.01 ± 0.01	0.09 ± 0.08
Repeatability (X_1–X_2)									
No-TCM	0.06 ± 0.04	0.03 ± 0.03	0.02 ± 0.01	0.10 ± 0.04	**0.17 ± 0.09**	0.11 ± 0.03	**0.37 ± 0.25**	0.01 ± 0.01	0.03 ± 0.01
Low-dose	0.05 ± 0.05	0.10 ± 0.10	0.03 ± 0.03	0.21 ± 0.23	**0.21 ± 0.15**	0.21 ± 0.26	**0.42 ± 0.45**	0.01 ± 0.01	0.07 ± 0.07
Ultralow-dose	0.02 ± 0.02	0.09 ± 0.11	0.06 ± 0.04	0.15 ± 0.15	**0.24 ± 0.16**	0.14 ± 0.17	**0.67 ± 0.50**	0.01 ± 0.01	0.05 ± 0.05
Sn ultralow-dose	0.05 ± 0.03	0.12 ± 0.12	0.06 ± 0.05	0.30 ± 0.25	**0.31 ± 0.14**	0.21 ± 0.16	**0.59 ± 0.16**	0.01 ± 0.01	0.09 ± 0.08

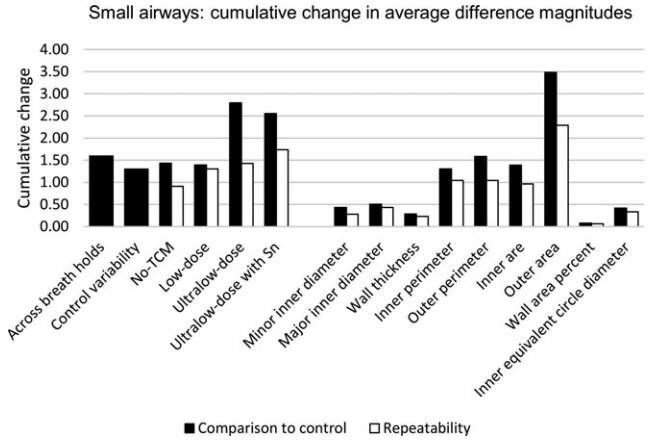

FIG. 3. Specific airway results for small airways. Cumulative change in average difference magnitudes for small airways showing normal variability across breath holds and within the control protocol. Results are presented with differences compared to control (black) and showing repeatability (white) and summed across measurement to assess by protocol (left) and summed across protocol to assess by measurement (left).

3.C.2. Medium airways

For medium airways, only minor inner diameter, wall thickness, and wall area percent did not appear to be affected by protocol when compared to equivalent results in the control variability protocol. The remaining airway measures — major inner diameter, inner and outer perimeter, inner and outer area, and inner equivalent circle diameter — showed average difference measures similar to those seen across breath holds (and larger than differences within the control variability set) in all protocols. Similar to small airways, outer area showed the highest deviations from the control; unlike small airways, inner area had the second highest deviations. It is important to note that deviations from the control protocol tended to increase as the raw measurement increased, as listed in Tables IV and V for both small and medium airways; therefore, larger differences, as observed for medium airways compared to small airways, may not always be an indicator of unreliability.

Repeatability of medium airways was observed to be affected by the tin-filtered ultralow-dose protocol, specifically when measuring outer area. In addition, the tin-filtered ultralow-dose protocol showed trends of overestimation of medium airway measures, similar to those seen in small airways. In comparison, the absence of TCM tended to underestimate medium airway measurements when compared to the control protocol with TCM. For medium airways, average difference magnitudes are displayed in Table V with cumulative change plots shown in Fig. 4.

4. DISCUSSION

This study found that quantitative airway and parenchymal measurements were comparable for low- and ultralow-dose protocols with the use of IR (ADMIRE). Work has previously been done validating noise levels and volume quality across doses with the incorporation of TCM and/or reconstruction methods.[33–37] Our work incorporated these techniques and focused on quantitative parenchymal and airway measurements with differences measured between each protocol and the control protocol, in a biologically relevant large animal model. Overall, diameter measurements, wall thickness, and

TABLE V. Specific airway results for medium airways. Average difference magnitudes for the four analyzed medium airways showing comparison of differences between each target scan and control scan acquired within the same breath hold (comparison to control) and differences between each target scan acquired within the same breath hold to assess for repeatability of airway measures (repeatability). Across breath hold differences are obtained between each control scan and the control scan acquired for the control variability set. Raw measurements were calculated from the airway measures obtained across each control scan. Results are presented as average difference magnitudes ± standard deviation. Bold indicates results showing the largest average difference magnitudes in comparison to control and across breath holds.

	Minor inner diameter (mm)	Major inner diameter (mm)	Wall thickness (mm)	Inner perimeter (mm)	Outer perimeter (mm)	Inner area (mm^2)	Outer area (mm^2)	Wall area Percent	Inner equivalent circle diameter (mm)
Raw measurement	5.70 ± 0.35	7.02 ± 0.49	1.30 ± 0.04	20.29 ± 1.5	28.64 ± 1.68	31.56 ± 4.27	**63.39 ± 6.58**	0.50 ± 0.02	6.46 ± 0.48
Across breath holds	0.14 ± 0.12	0.28 ± 0.17	0.03 ± 0.02	0.62 ± 0.59	0.72 ± 0.58	1.74 ± 1.25	**2.87 ± 2.09**	0.01 ± 0.01	0.20 ± 0.19
Control variability	0.16 ± 0.15	0.10 ± 0.11	0.04 ± 0.02	0.12 ± 0.09	0.24 ± 0.24	0.54 ± 0.39	**0.89 ± 0.72**	0.01 ± 0.01	0.04 ± 0.03
Comparison to control ($X_{1/2}$–X_c)									
No-TCM	0.07 ± 0.06	0.17 ± 0.18	0.06 ± 0.03	0.59 ± 0.76	0.63 ± 0.70	1.15 ± 1.11	**2.03 ± 1.98**	0.01 ± 0.01	0.19 ± 0.24
Low-dose	0.10 ± 0.05	0.10 ± 0.08	0.04 ± 0.05	0.17 ± 0.19	0.45 ± 0.33	0.50 ± 0.54	**1.72 ± 1.32**	0.01 ± 0.01	0.06 ± 0.06
Ultralow-dose	0.08 ± 0.05	0.14 ± 0.15	0.02 ± 0.02	0.25 ± 0.29	0.45 ± 0.39	0.68 ± 0.79	**1.78 ± 1.57**	0.01 ± 0.00	0.08 ± 0.09
Sn ultralow-dose	0.10 ± 0.08	0.24 ± 0.34	0.03 ± 0.03	0.63 ± 1.14	0.70 ± 0.91	1.12 ± 1.66	**2.17 ± 2.32**	0.01 ± 0.01	0.20 ± 0.36
Repeatability (X_1–X_2)									
No-TCM	0.02 ± 0.01	0.04 ± 0.03	0.02 ± 0.02	0.03 ± 0.01	0.18 ± 0.19	0.04 ± 0.05	**0.61 ± 0.61**	0.00 ± 0.01	0.01 ± 0.00
Low-dose	0.09 ± 0.04	0.08 ± 0.04	0.01 ± 0.02	0.20 ± 0.15	0.28 ± 0.22	0.51 ± 0.46	**0.99 ± 0.89**	0.01 ± 0.00	0.06 ± 0.05
Ultralow-dose	0.07 ± 0.03	0.13 ± 0.14	0.03 ± 0.02	0.17 ± 0.29	0.49 ± 0.21	0.46 ± 0.62	**1.68 ± 0.97**	0.01 ± 0.01	0.05 ± 0.09
Sn ultralow-dose	**0.08 ± 0.09**	**0.46 ± 0.53**	**0.06 ± 0.04**	**1.21 ± 1.49**	**1.36 ± 1.33**	**2.06 ± 2.04**	**4.22 ± 3.41**	**0.01 ± 0.00**	**0.38 ± 0.47**

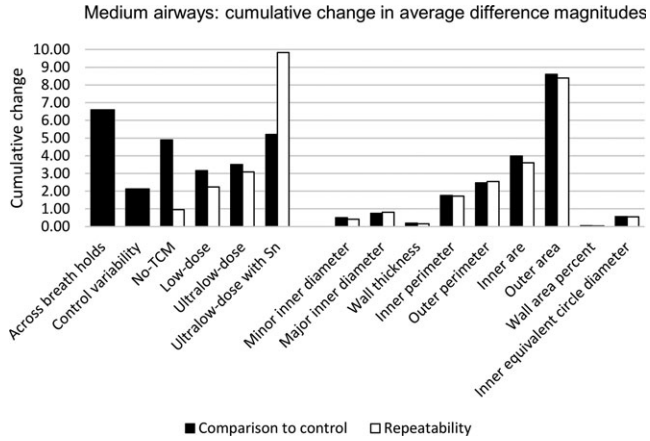

FIG. 4. Specific airway results for medium airways. Cumulative change in average difference magnitudes for medium airways showing normal variability across breath holds and within the control protocol. Results are presented with differences compared to control (black) and showing repeatability (white) and summed across measurement to assess by protocol (left) and summed across protocol to assess by measurement (left).

derived measures (wall area fraction, inner equivalent circle diameter) were the most reliable and repeatable airway measures, where larger differences were observed for area and perimeter measurements. Comparable airway measures were observed across the no-TCM, low-dose, and both ultralow-dose protocols with trends indicating ultralow-dose protocols have greater difference magnitudes (similar to variability in measurements seen across breath holds). Additionally, small airways showed smaller differences from control compared to medium airways. This may be explained as the magnitude of small airway differences across all measurements and protocols were subvoxel on average (0.23 mm ± 0.25).

The validation of quantitative measures across scanner protocols and reconstruction methods is important due to the increased use of quantitative lung CT in disease characterization in large, multicenter trials. The current protocol for NIH-SPIROMICS does not include IR during reconstruction due to the significant differences reported in acquired emphysema and airway measures between volumes obtained with and without IR.[18,38,39] In comparison, our laboratory showed satisfactory quantitative attenuation measures at doses comparable to chest x-ray (0.15 mGy) with the use of a newer version of IR (ADMIRE) and a tin filter on a SOMATOM Force scanner with the use of a test object.[23] We also found comparable mean density measures across several doses with IR; however, deviations in emphysema measures (% < −910 HU and % < −950 HU) were observed at ultralow-doses with greater severity in differences observed in the tin-filtered ultralow-dose protocol. In addition, the tin-filtered ultralow-dose protocol showed systematic overestimation of airway measurements. It is important to note that the two ultralow-dose protocols included in this study were independently constructed to achieve CTDIvols < 1 mGy. The difference between the two protocols incorporates tin filtering, and also includes different kV and mAs. While large reductions in CTDIvol were achieved, these trends indicate further need for studies to understand the effect of spectral shaping on airway and parenchymal measures, using related protocols examining solely the impact of tin filtering (excluding other variables).

Additionally, we compared protocols with and without the use of TCM. Similar to IR, the NIH-SPIROMICS protocol

does not use TCM. At the time that the SPIROMICS protocol was originally established, TCM technology was new and less refined than that in the current CT systems and did cause some nonuniformity throughout the lungs (data not published). In our study, we found the absence of TCM to produce the most repeatable results, as we were examining measures within the same subject. However, inclusion of TCM is expected to have benefit in multicenter studies across variable-sized subjects, whereby noise is held constant. We did find a systematic underestimation of airway measurements compared to the equivalent protocol with the use of TCM (control), specifically among the analyzed medium airways.

Airway wall thickness as measured through quantitative analysis of CT data, has been utilized as a metric to understand the etiology of COPD.[29,40,41] Recent work has shown that greater airway wall thickening, represented by pi10, is an early indicator of disease in symptomatic current or former smokers with normal spirometry.[30] With the use of low- and ultralow-dose protocols, our results showed consistency across pi10 measurements, even with variability in number of airways segmented. This trend was observed before and after merging of fractured airway branch paths for consistency across all airway trees. In addition to the merging of airway branches, editing of airway trees included seed point placement to grow out the base of the airway trees due to the differences between human and pig lungs[42]; however, all segmentation was automatically performed with the Apollo software. The least number of segmented airways was observed in the control protocol variability set; however, this set showed the smallest lung volume at approximately 200 mL less than the remaining scans. It is well known that lung volume has an effect on quantitative density measures with normalizations developed to compensate for differences in volume across breath holds.[43] Therefore, we compared results taken from volumes within the same breath hold; however, variability was still observed within the control variability set despite mechanical enforcement. To minimize this limitation, we used the control and first target volume to acquire difference measures for comparison. It can be seen that over the course of the study sets, the number of airway branches segmented in the control protocol increased and closely reflected, or was higher than the number of airway branches segmented in the two target scans acquired within the same breath hold.

Furthermore, we also explored additional airway measurements, including those previously used for correlation with COPD GOLD stage in large, multicenter trials.[41,44] We found that area and perimeter measurements, specifically of the outer airway component, are less reliable, while diameter measurements and wall thickness produced were more reliable and repeatable. Derived measures (wall area percent, inner equivalent circle diameter) also showed reliability and repeatability; however, wall area fraction is derived from inner and outer areas which demonstrated the largest differences and inner equivalent circle diameter is derived from inner perimeter showing the same differences simply scaled by pi. While these derived measures are consistent across protocols in this study, they may not be reliable biomarkers of structural change, as they are scaled parameters calculated from measurements susceptible to protocol variability and repeatability.

Our study was limited through the use of a single large animal subject, studied repeatedly with different protocols. Extrapolation of our results to comparisons across subjects and time points may be minimal, although our findings in this biological model support those of similar studies performed using test objects.[23,39] As a baseline measure of variability, we compared measurements across breath holds; however, no corrections were made to compensate for inspiratory volume differences,[43] which ranged from 1.7 to 2.1 L despite mechanically enforced breath holds. This reflects a significant challenge of consistent inspiratory lung volume for repeated measures, also encountered in clinical studies incorporating quantitative CT measures for lung assessment.[12] Research has also shown that quantitative parenchymal measures differ by lobe.[45] Due to the lobar structure of pig lungs and additional segmentation required, a comprehensive analysis of the animal's lung lobes was not included in this study.[42]

5. CONCLUSIONS

In conclusion, the use of IR with low- and ultralow-dose CT protocols with CT volume dose indices down to 0.32 mGy maintains selected quantitative parenchymal and airway measurements relevant to multicenter trials. Mean parenchymal measures, including median and standard deviation, were preserved in the presence of ultralow-dose and tin-filtered ultralow-dose dose protocols; however, limited reliability was seen in emphysema measures (% < -910 HU) for the included ultralow-dose dose protocols. Reliability was observed across wall thickness and major and minor diameter airway measures compared to area and perimeter measurements with respect to the variability seen in the control protocol. Specifically, caution should be used if using outer area as an important quantitative measure of the airways. Importantly, derived airway measurements showed consistency across all protocols; however, they are dependent on measurements that demonstrated the largest differences. Lastly, more studies are required to further understand the effect spectral shaping with tin filtering and TCM have on quantitative parenchymal and airway measures.

ACKNOWLEDGMENTS

This research was supported in part by the NIH grant R01 HL112986 and S10 OD018526.

CONFLICTS OF INTEREST

E.A.H. is a founder and shareholder of VIDA Diagnostics, Inc. a company commercializing lung image analysis software developed, in part, at the University of Iowa. J.D.N. is a

paid consultant for VIDA Diagnostics, Inc. and has stock options in the company. J.C.S. has VIDA Diagnostics, Inc. stock options. J.P.S. is an employee and shareholder in VIDA Diagnostics, Inc. Siemens Healthcare has provided in-kind support for hardware and software residing at the University of Iowa and used in this project.

[a]Author to whom correspondence should be addressed. Electronic mail: jessica-sieren@uiowa.edu; Telephone: (319) 356-1407.

REFERENCES

1. Niimi A, Matsumoto H, Amitani R, et al. Airway wall thickness in asthma assessed by computed tomography. Relation to clinical indices. *Am J Respir Crit Care Med*. 2000;162:1518–1523.
2. Busacker A, Newell JD Jr., Keefe T, et al. A multivariate analysis of risk factors for the air-trapping asthmatic phenotype as measured by quantitative CT analysis. *Chest*. 2009;135:48–56.
3. Aysola RS, Hoffman EA, Gierada D, et al. Airway remodeling measured by multidetector CT is increased in severe asthma and correlates with pathology. *Chest*. 2008;134:1183–1191.
4. Montaudon M, Lederlin M, Reich S, et al. Bronchial measurements in patients with asthma: comparison of quantitative thin-section CT findings with those in healthy subjects and correlation with pathologic findings. *Radiology*. 2009;253:844–853.
5. Besir FH, Mahmutyazicioglu K, Aydin L, Altin R, Asil K, Gundogdu S. The benefit of expiratory-phase quantitative CT densitometry in the early diagnosis of chronic obstructive pulmonary disease. *Diagn Interv Radiol (Ankara, Turkey)*. 2012;18:248–254.
6. Xie X, de Jong PA, Oudkerk M, et al. Morphological measurements in computed tomography correlate with airflow obstruction in chronic obstructive pulmonary disease: systematic review and meta-analysis. *Eur Radiol*. 2012;22:2085–2093.
7. Lynch DA, Al-Qaisi ML. Quantitative CT in COPD. *J Thorac Imaging*. 2013;28:284–290.
8. Zach JA, Newell JD, Schroeder J, et al. Quantitative CT of the lungs and airways in healthy non-smoking adults. *Invest Radiol*. 2012;47:596–602.
9. Mets OM, de Jong PA, van Ginneken B, Gietema HA, Lammers JWJ. Quantitative computed tomography in COPD: possibilities and limitations. *Lung*. 2012;22:2103–2109.
10. Newell JD, Sieren J, Hoffman EA. Development of quantitative CT lung protocols. *J Thorac Imaging*. 2013;28:226–271.
11. Couper D, LaVange LM, Han M, et al. Design of the subpopulations and intermediate outcomes in COPD study (SPIROMICS). *Thorax*. 2014;69:492–495.
12. Sieren JP, Newell JD Jr., Barr RG, et al. SPIROMICS protocol for multicenter quantitative computed tomography to phenotype the lungs. *Am J Respir Crit Care Med*. 2016;194:794–806.
13. Kalender WA, Wolf H, Suess C. Dose reduction in CT by anatomically adapted tube current modulation. II. Phantom measurements. *Med Phys*. 1999;26:2248–2253.
14. Kalra MK, Maher MM, Toth TL, et al. Techniques and applications of automatic tube current modulation for CT. *Radiology*. 2004;233:649–657.
15. McCollough CH, Bruesewitz MR, Kofler JM. CT dose reduction and dose management tools: overview of available options. *Radiographics*. 2006;26:503–512.
16. Gies M, Kalender WA, Wolf H, Suess C. Dose reduction in CT by anatomically adapted tube current modulation. I. Simulation studies. *Med Phys*. 1999;26:2235–2247.
17. Hara AK, Paden RG, Silva AC, Kujak JL, Lawder HJ, Pavlicek W. Iterative reconstruction technique for reducing body radiation dose at CT: feasibility study. *Am J Roentgenol*. 2009;193:764–771.
18. Mets OM, Willemink MJ, de Kort FP. The effect of iterative reconstruction on computed tomography assessment of emphysema, air trapping and airway dimensions. *Eur Radiol*. 2012;22:2103–2109.
19. Beister M, Kolditz D, Kalender WA. Iterative reconstruction methods in X-ray CT. *Physica Med*. 2012;28:94–108.
20. Gordic S, Morsbach F, Schmidt B, et al. Ultralow-dose chest computed tomography for pulmonary nodule detection: first performance evaluation of single energy scanning with spectral shaping. *Invest Radiol*. 2014;49:465–473.
21. Stolzmann P, Leschka S, Scheffel H, et al. Characterization of urinary stones with dual-energy CT: improved differentiation using a tin filter. *Invest Radiol*. 2010;45:1–6.
22. Weis M, Henzler T, Nance JW Jr., et al. Radiation dose comparison between 70 kVp and 100 kVp with spectral beam shaping for non-contrast-enhanced pediatric chest computed tomography: a prospective randomized controlled study. *Invest Radiol*. 2017;52:155–162.
23. Newell JD Jr., Fuld MK, Allmendinger T, et al. Very low-dose (0.15 mGy) chest CT protocols using the COPDGene 2 test object and a third-generation dual-source CT scanner with corresponding third-generation iterative reconstruction software. *Invest Radiol*. 2015;50:40.
24. Regan EA, Hokanson JE, Murphy JR, et al. Genetic epidemiology of COPD (COPDGene) study design. *COPD*. 2010;7:32–43.
25. Jarjour NN, Erzurum SC, Bleecker ER, et al. Severe asthma: lessons learned from the National Heart, Lung, and Blood Institute Severe Asthma Research Program. *Am J Respir Crit Care Med*. 2012;185:356–362.
26. Barr RG, Ahmed FS, Carr JJ, et al. Subclinical atherosclerosis, airflow obstruction and emphysema: the MESA lung study. *Eur Respir J*. 2012;39:846.
27. Grydeland TB, Dirksen A, Coxson HO, et al. Quantitative computed tomography: emphysema and airway wall thickness by sex, age and smoking. *Eur Respir J*. 2009;34:858–865.
28. Nakano Y, Wong JC, deJong PA. The prediction of small airway dimensions using computed tomography. *Am J Respir Crit Care Med*. 2005;171:142–146.
29. Grydeland TB, Dirksen A, Coxson HO, et al. Quantitative computed tomography measures of emphysema and airway wall thickness are related to respiratory symptoms. *Am J Respir Crit Care Med*. 2010;181:353–359.
30. Woodruff PG, Barr RG, Bleecker E, et al. Clinical significance of symptoms in smokers with preserved pulmonary function. *N Engl J Med*. 2016;374:1811–1821.
31. Dournes G, Laurent F, Coste F, et al. Computed tomographic measurement of airway remodeling and emphysema in advanced chronic obstructive pulmonary disease. Correlation with pulmonary hypertension. *Am J Respir Crit Care Med*. 2015;191:63–70.
32. Guo J, Fuld M, Alford S, Reinhardt J, Hoffman E. Pulmonary Analysis Software Suite 9.0: integrating quantitative measures of function with structural analyses. Proceedings of the First International Workshop on Pulmonary Image Analysis; 2008:283-292.
33. Bucher AM, Kerl MJ, Albrecht MH, et al. Systematic comparison of reduced tube current protocols for high-pitch and standard-pitch pulmonary CT angiography in a large single-center population. *Acad Radiol*. 2016;23:619–627.
34. Greess H, Wolf H, Baum U, et al. Dose reduction in computed tomography by attenuation-based on-line modulation of tube current: evaluation of six anatomical regions. *Eur Radiol*. 2000;10:391–394.
35. Greess H, Nomayr A, Wolf H, et al. Dose reduction in CT examination of children by an attenuation-based on-line modulation of tube current (CARE Dose). *Eur Radiol*. 2002;12:1571–1576.
36. Tack D, De Maertelaer V, Gevenois PA. Dose reduction in multidetector CT using attenuation-based online tube current modulation. *Am J Roentgenol*. 2003;181:331–334.
37. Scholtz JE, Wichmann JL, Husers K, et al. Automated tube voltage adaptation in combination with advanced modeled iterative reconstruction in thoracoabdominal third-generation 192-slice dual-source computed tomography: effects on image quality and radiation dose. *Acad Radiol*. 2015;22:1081–1087.
38. Choo JY, Goo JM, Lee CH, Park CM, Park SJ, Shim M-S. Quantitative analysis of emphysema and airway measurements according to iterative reconstruction algorithms: comparison of filtered back projection, adaptive statistical iterative reconstruction and model-based iterative reconstruction. *Eur Radiol*. 2014;24:799–806.

39. Sieren JP, Hoffman EA, Fuld MK, Chan KS, Guo J, Newell JD Jr. Sinogram affirmed iterative reconstruction (SAFIRE) versus weighted filtered back projection (WFBP) effects on quantitative measure in the COPDGene 2 test object. *Med Phys*. 2014;41:091910.
40. Patel BD, Coxson HO, Pillai SG. Airway wall thickening and emphysema show independent familial aggregation in chronic obstructive pulmonary disease. *Am J Respir Crit Care Med*. 2008;178:500–505.
41. Smith BM, Hoffman EA, Rabinowitz D, et al. Comparison of spatially matched airways reveals thinner airway walls in COPD. The Multi-Ethnic Study of Atherosclerosis (MESA) COPD Study and the Subpopulations and Intermediate Outcomes in COPD Study (SPIROMICS). *Thorax*. 2014;69:987–996.
42. Swindle MM, Makin A, Herron AJ, Clubb FJ Jr., Frazier KS. Swine as models in biomedical research and toxicology testing. *Vet Pathol*. 2012;49:344–356.
43. Pompe E, van Rikxoort EM, Mets OM, et al. Follow-up of CT-derived airway wall thickness: correcting for changes in inspiration level improves reliability. *Eur J Radiol*. 2016;85:2008–2013.
44. Washko GR, Diaz AA, Kim V, et al. Computed tomographic measures of airway morphology in smokers and never-smoking normals. *J Appl Physiol*. 2014;116:668–673.
45. Schroeder JD, McKenzie AS, Zach JA, et al. Relationships between airflow obstruction and quantitative CT measurements of emphysema, air trapping, and airways in subjects with and without chronic obstructive pulmonary disease. *AJR Am J Roentgenol*. 2013;201:W460–W470.